

New-generation hexabundles: development and initial results

Rebecca Brown^{a,b,c,*}, Adeline H. Wang^{a,b,c,*}, Julia J. Bryant^{a,b,c}, and Sergio Leon-Saval^a

^aSchool of Physics, The University of Sydney, NSW 2006, Australia;

^bAustralian Astronomical Observatory, Faculty of Science and Engineering, Macquarie University, NSW 2109, Australia

^cARC Centre of Excellence for All Sky Astrophysics in 3 Dimensions (ASTRO 3D)

ABSTRACT

The original optical fibre imaging bundles called ‘hexabundles’ have proven to be exceptionally effective in the Sydney-AAO Multi-object IFS (SAMI) instrument, enabling one of the worlds largest IFS galaxy surveys^{5,6}. We are now developing an improved next-generation hexabundle design. These IFUs use a novel assembly technique developed in the Sydney Astrophotonic Instrumentation Laboratories (SAIL) at the University of Sydney, that enable very high fill-fraction and an evenly distributed, hexagonally packed, array of 217 fibre cores. These new hexabundles will see first light in 2019 on the new Hector-I instrument for the Anglo-Australian Telescope (AAT). The large number of fibre cores will measure spatially-resolved spectroscopy of galaxies out to 2 effective radii. The hexabundles are currently being prototyped, and characterised. The impact of the hexagonal packing of the fibre cores on Focal Ratio Degradation (FRD), total throughput of the device and overall performance will be presented.

Keywords: hexabundles, integral field units, Hector, optical fibres, fibre positioner, AAT, spectroscopy

1. INTRODUCTION

Hector is the next generation spectrograph for integral field spectroscopy at the Anglo-Australian Telescope (AAT). The instrument is an upgrade to the highly productive Sydney-AAO Multi-object IFS (SAMI) instrument^{3,6}, which has produced over 40 papers and captured data of over 3000 galaxies during its 5 year lifetime. Hector I will be on sky in 2019A, and will include 21 integral field units (IFUs) called hexabundles¹⁻⁴ that will cover up to 30 arcseconds on sky, out to 2 effective radii (R_e) of most galaxies. It will build on the success of SAMI, enabling a 15,000 galaxy survey on the AAT. The instrument will be installed on the 2 degree field top end of the AAT, and will use robotically-positioned magnetic connectors to locate the IFUs on the field plate before the observation of each field. This paper will describe the development and first results of the hexagonal hexabundle IFUs. A separate paper (see Bryant et al.; Paper 10702-53) gives an overview of the complete Hector instrument and a third paper (see Content et al.; Paper 10702-312) details the Hector spectrograph design.

The new generation of hexabundles differ in a number of ways from the SAMI hexabundles. While the SAMI hexabundles were circular and all the same size of 61 fibres, the Hector hexabundles will vary in size from 61 to 217 fibres, and be packed in a hexagonal array. See Table 1 for a summary of the comparison between these two designs. The fill fraction (ratio of fibre core to total IFU size) of the SAMI hexabundles, is approximately 75%. This is 50% higher fill fraction than any other fibre IFUs for astronomy. The hexagonal hexabundles will have a slightly higher fill fraction, because of their regularly packed array. This regular array will be invaluable to the surveys, due also to its significant ease in data reduction, and more efficient calibration.

The most notable difference from the SAMI hexabundles will be in the array of sizes. The sizes have been chosen to measure most galaxies in the Hector Survey out to $2R_e$. The largest hexabundles will have a 30 arcsecond diameter. This is almost twice the diameter of the SAMI hexabundles and so gives a far greater view

* Correspondance to: rbrown9155@uni.sydney.edu.au, hwan5380@uni.sydney.edu.au.

† These authors contributed equally to the work.

Instrument	SAMI	HECTOR
Packing Profile	Circular	Hexagonal
No. fibre Cores	61	61, 91, 127, 169, 217
fibre Diameter(core/cladding)	105/110mm	103/108mm
Fill Fraction	75%	>75%
Focal plane field of view diameter	1 degree	2 degrees

Table 1: Comparison of the improvements between SAMI and next generation instrument Hector.

to understand phenomena such as galaxy mergers, star formation histories, and galaxy dynamics in some of the larger galaxies, for which SAMI only samples the galaxy centre. Figure 1 shows the SAMI hexabundle alongside an indicative image of the largest size hexabundle over a galaxy, and a microscope image of the latest 61-fibre hexagonal hexabundle.

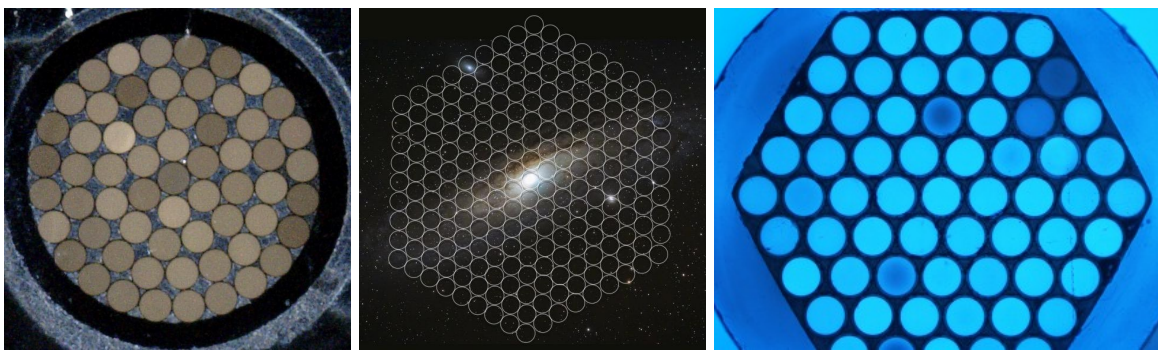


Figure 1: The left image shows a SAMI bundle which has a circular packing. The centre image is indicative of the largest hexagonal IFU that will be built for Hector, superimposed over a galaxy to show its position on sky. The right image shows a 61-core hexagonally packed new generation hexabundle that has been tested for results in this paper. It has a consistent and regular array of fibres which ensures simplified calibration and data reduction. The cores are randomly illuminated for the image.

This paper will describe in Section 2, the current hexabundles and important variables that have been considered throughout their production. Section 3 will describe some of the most recent results that we have had from these hexabundles, including a detailed analysis of the FRD measurements. Finally, we will conclude in Section 4, with a summary of the current status.

2. HEXABUNDLE ASSEMBLY

The optical fibre fusing process that was developed for the SAMI hexabundles has undergone some development to allow for the hexagonally packed arrays of the new Hector hexabundles. The new fibre fusing process must optimise the tight and even fibre packing to give a consistent 75% fill fraction. The fibre cladding is etched to $5\mu\text{m}$ thickness over a short length, to increase the fill fraction. The packed and fused fibre bundle is carefully glued into a custom designed ferrule, that will protect the bundle while it is being positioned on the focal surface in the AAT. The core considerations in this development process is to build hexabundles that are evenly and tightly packed, in an extremely consistent array while maintaining the optical performance of individual fibres. It is imperative to the galaxy surveys that minimal focal ratio degradation is induced throughout this process, so care has been taken to reduce this in each step.

The etching of the fibres is a process that is being developed in conjunction with the Sydney Nanoscience Hub, the University of Sydney node of the Australian National Fabrication Facility Network (ANFF). Some work has gone into developing a consistent process, to ensure an extremely consistent etch on each of the fibres. Each fibre will have its buffer stripped off and then the cladding etched to $5\mu\text{m}$ thick with a low concentration of hydrofluoric acid. This thickness is only needed over the short length that they are packed into the hexabundle, and so must be etched, rather than purchasing fibre with thinner cladding. The high fill fraction and regularity of the array in the hexabundle depend on there being very low deviation from fibre-to-fibre in the thickness of the cladding.

One of the first prototypes of the new Hector hexabundles is shown in Figure 1 (right). Fusing of optical fibres leads to FRD. However our unique process has been carefully optimised with an aim for the FRD in the final hexabundle to be no worse than that of the bare fibre it is made from. Section 3 will compare the FRD performance of this bundle to bare fibre.

These fused hexabundles are installed into the instrument at 90 degrees to the focal plane. They lie along the field plate, at any position across the 2-degree-diameter focal plane. To redirect light from the primary mirror into the hexabundle there will be a prism attached to each hexabundle face. The fibres coming out of the back of the ferrule will be spliced to the 40m fibre cable, which will route to the Hector spectrograph.

3. PERFORMANCE

3.1 Method for testing FRD

When light is input into a fibre at a particular cone angle, the light from the other end will come out of the fibre at a larger cone angle. This is called Focal Ratio Degradation, and is a result of modal coupling within the fibre due to small imperfections, bends and impurities in the fibre, and the end finish.⁸ FRD is improved for lower f-ratio input light, and therefore optical fibre instruments are ideal when the f-ratio from the telescope is $f/\sim 4$.^{4,7} If the light coming out of the fibre has a cone angle larger than the acceptance angle of the spectrograph then light will be lost from the system. Therefore it is important to optimise the system to reduce FRD. In Hector, the spectrograph acceptance cone is slightly bigger than the input light cone to further protect against light loss. In testing the FRD of the Hector prototype hexabundles, we used an $f/3.4$ ($\text{NA}=0.147$) input beam to match the input f-ratio into the hexabundle fibres from the AAT 2-degree field top end.

To define the quality of the hexabundle we achieved, we need to test the FRD of representative fibres in each ring of the hexabundle pattern, then compare it to a single bare fibre. To test the FRD of a single bare fibre, we built an optical setup for measuring both the input and the output light (shown in Fig. 2). We used a Mightex fibre-coupled white light LED source as the input light and we set the power of the light consistently as 600mA for each measurement. An SMF-28 fibre patch cord from the light source was aligned to a 75mm convex achromat lens to collimate the light from the source. An aperture in the collimated beam then adjusted the beam width to create an $f/3.4$ beam out of the 35mm focal length refocussing lens. An additional aim of the aperture was to allow through light from just the top of the light profile from the fibre in order to give an approximately flat-topped beam. Two Bessell filters in a filter wheel within the collimated beam were used in turn, centered on blue ($\sim 457\text{nm}$) and red ($\sim 596\text{nm}$) wavelengths. The image taken at the focus shows that the diameter of the spot at focus is $48.6\mu\text{m}$, which is ideal for feeding all the input light into the fibre without cross-talk to adjacent fibres, because it is much smaller than the fibre core size of $103\mu\text{m}$. Photos of the setup are shown in Fig. 3.

To measure the input light fed into our fibres, we removed the hexabundle holder and imaged the $f/3.4$ beam directly (see the lower left image in Fig. 3). When we tested a single bare fibre, it was mounted in an SMA connector in the hexabundle holder, and the output end of the fibre lay along a v-groove (see the lower right image in Fig. 3). The fibre end was placed very gently with light tape because any slight pressure on the fibre will cause bad FRD. A CCD was placed at several far-field positions to take images of the output light from the bare fibre directly. For hexabundles, the measuring method was the same and the hexabundle pigtailed were mounted in the v-groove. In each case a vision system on the side of the input setup allowed the incoming $f/3.4$ beam to be accurately focussed and centred on the fibre being tested.

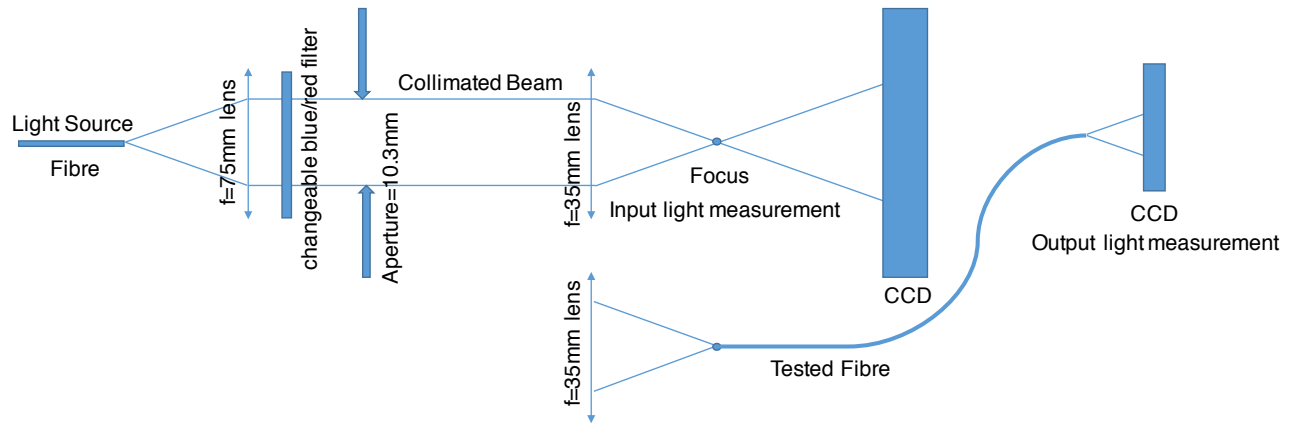


Figure 2: Diagram of the testing setup: illustrating from the left to the right the SMF-28 fibre from the LED light source, 75mm convex lens (vertical arrow), blue/red filters in a filter wheel, aperture iris, 35mm convex lens (vertical arrow), fibres for testing and CCD.

3.2 Measurement Error

During the measurement and calculation process, there are various errors coming from the alignment precision of the testing apparatus, fitting uncertainties on the images and so on, which will influence the final FRD result. These errors include the alignment of the stages, the repositioning of the input and output fibre holders, then placement of the fibre in the v-groove and the focussing on the fibre face. Each of these were measured or estimated and then summed in quadrature to give the total error shown in the plot in Section 3.3.

It is notable that the code to fit the images was optimised after extensive testing, to minimise the impact on the measured FRD from the fitting. For example, to accommodate any ellipticity in the output light due to any slight misalignment of the CCD chip on-axis, our custom code fits an elliptical annulus at 95% of the image intensity. The centre of the fibre image profile is then fit from that ring. Repeated testing of this method has shown the error in the fitted image centre is negligible (see 2, first line). This is important as the NA output values measured from the image will be inflated if the centre is offset from its true position. Similarly, if the image background is not correctly accounted for in the fitting, then the NA will be measured to be artificially small. By optimising the code to improve the background fitting the error in the NA from this effect was reduced to < 0.001 .

Error	Value (measured in NA)
Center Fitting	0.000063
Background Fitting	< 0.001

Table 2: Errors from the fitting method adopted in our new code as discussed in the text.

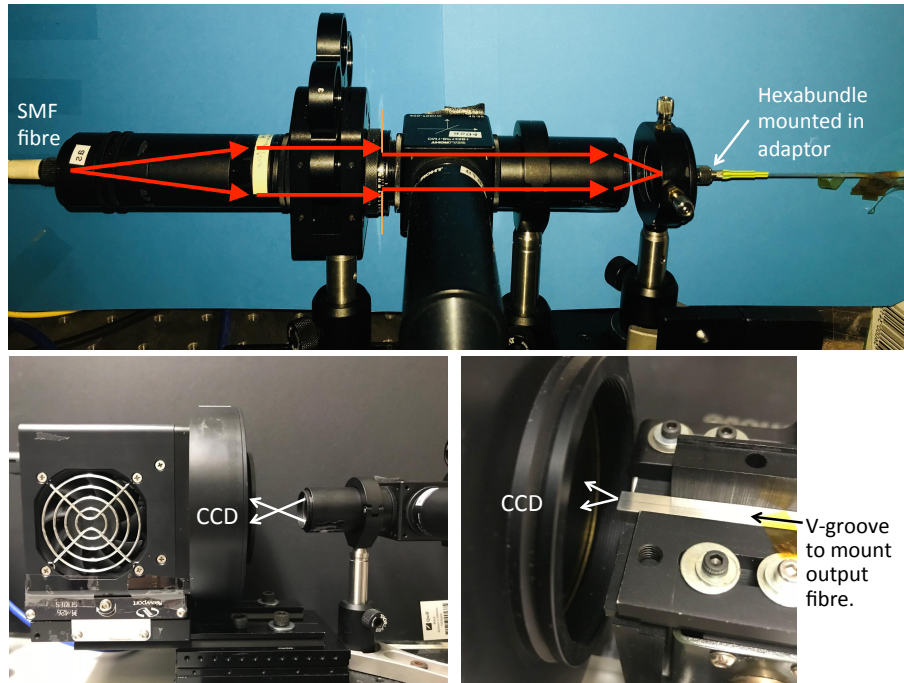


Figure 3: The top image shows the input setup illustrated in Fig. 2 feeding an F/3.4 beam into the hexabundle on the right-hand side. The lower left image is the CCD measuring the input light before it is fed into the hexabundle. The lower right image shows a fibre pigtail end that has come out of a hexabundle, lying on the v-groove in front of the CCD.

3.3 FRD Analysis

From the plot of NA versus encircled energy, we can see how the FRD influences the encircled energy (EE). If a fibre has worse FRD, its NA versus EE curve will shift to the right of the input curve. We note that the shape of the input curve will be sharper near the maximum EE because the input light was close to a top-hat function. However the fibres will couple that light between modes, meaning that at low radii in the image (low output NA angle) some light will couple inwards to lower order modes, but at high radii (typically where $EE > \sim 95\%$) there is natural coupling to higher order modes that rounds off the EE profile. That effect is not FRD, but instead FRD is evident when the rounded output curves shift further to the right. In Fig. 4, the output curve from different cores are very close to the input curve, which infers that all these cores have FRD that is very good. In particular, the hexabundle fibres from the centre three rings of the hexabundle have FRD as good as that of the single bare fibre, which demonstrates that the carefully crafted fusing process that is used to create the hexabundles does not introduce any FRD. It is noticeable however that the fibres tested from the outer two rings of the hexabundle had slightly worse FRD than the inner cores. While this difference is not significant within errors, we are working to improve on this because it is due to extra pressure on the outside of the hexabundle from the process and we can optimise further to remove that.

We made a cut in the NA-Encircled Energy plot at 80%, 90%, and 95% EE, then recorded the corresponding NA at each core as shown in Fig. 5. From the bare fibre to the fibres in each row of the hexabundle, the NA values are not changing within errors at a given EE. However, we can tell that the outer two cores are a little higher. This will be the main point for us to improve the next prototype.

The throughput of the hexabundles was measured by comparing the light input (within the equivalent f/3.40 of the AAT 2-degree field top end) and the output from the fibres (within the acceptance cone of the Hector spectrograph at f/3.264). The test hexabundles are not antireflection coated but the final hexabundles will be

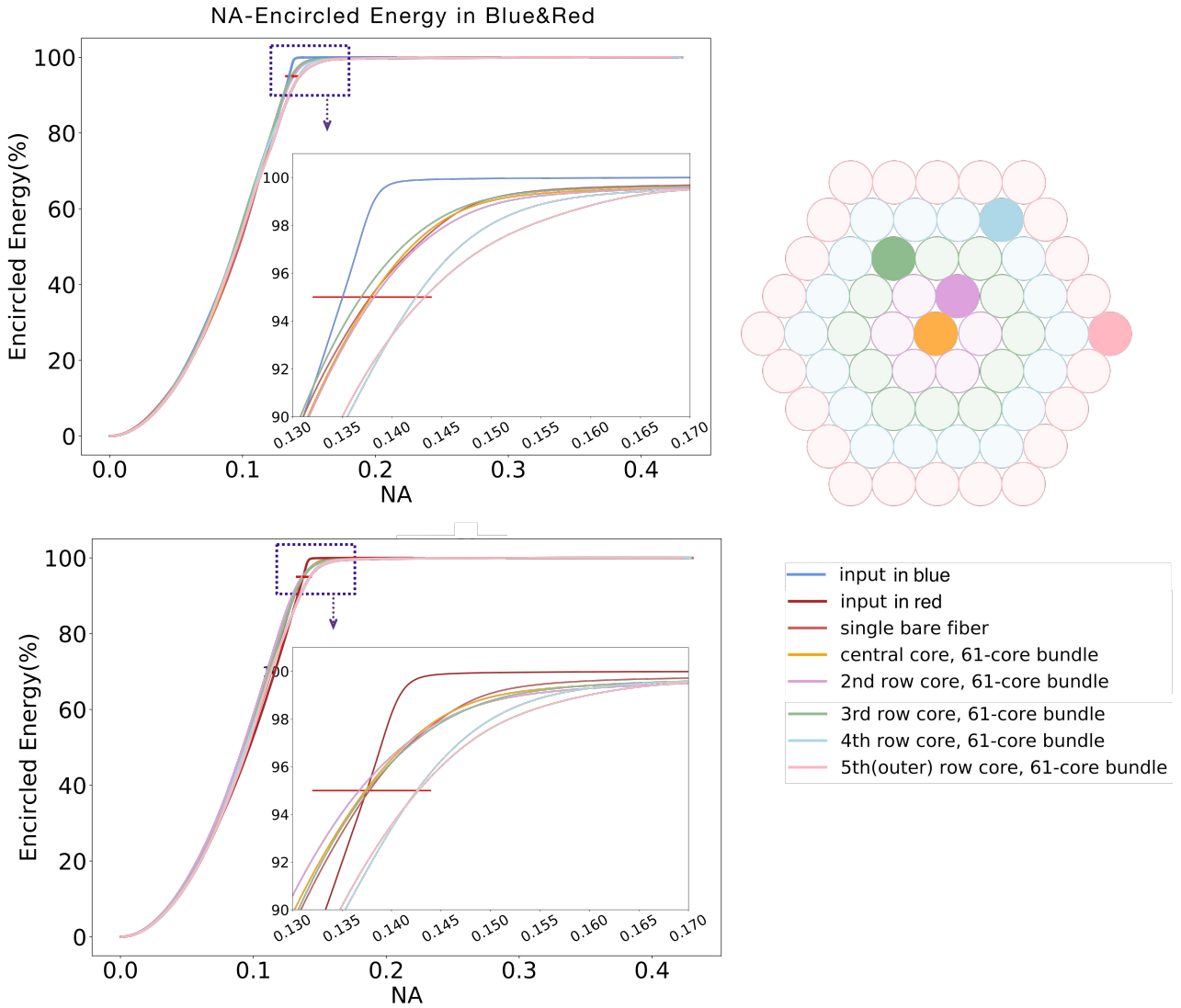


Figure 4: Encircled energy versus numerical aperture (NA) through the blue (top) and red (bottom) filters. FRD shifts the curves to the right. The output curves are more rounded than the input for $EE \lesssim 95\%$ due to modal transitions in the fibre. The hexabundle fibres show FRD as low as the same bare fibre (within errors [red bar]). This means the fusing technique to create the hexabundles successfully retains the optical properties of the fibres. There is a slight increase in the FRD in the two outermost rows, which we expect to be optimised in future prototypes.

and so a correction was made for the 3.3% reflection at the air/glass interface at either end of the fibres. The results in Table 3 show that the throughput performance is very good. The throughput is lower in the blue due to the transmission properties of the fibre, and the outer-most ring of cores have a slightly lower throughput due to the extra FRD discussed above.

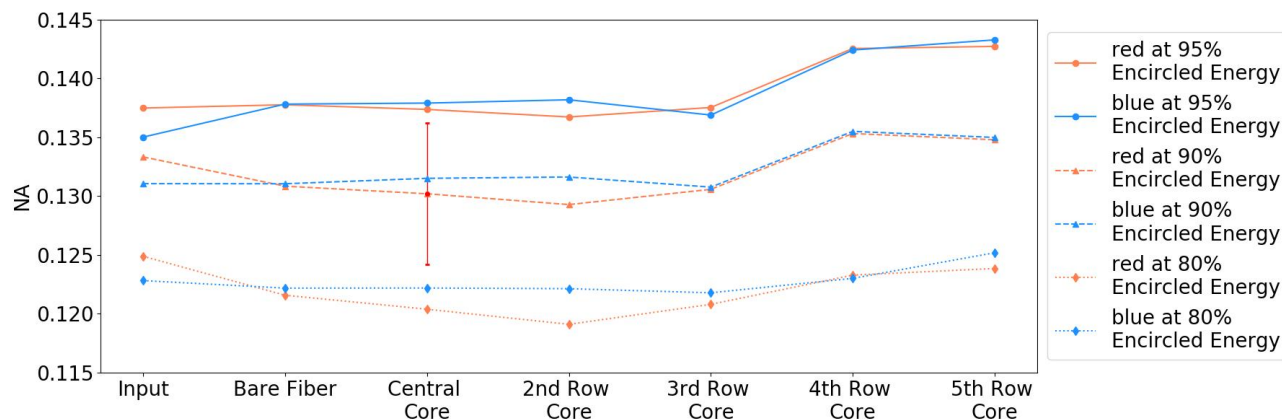


Figure 5: At EE levels of 80, 90 and 95%, the NA values are shown through the blue and red filters for each of the fibre cores measured. The hexabundle cores have no increase in FRD compared to the bare fibre within errors, but the outer two hexabundle rows show a slight, increase that can be improved with further optimisation. The red vertical line is the error bar.

Throughput(%)	Central Core	2nd Row Core	3rd Row Core	4th Row Core	5th Row Core
Red	95.05	93.66	98.30	95.32	93.20
Blue	93.13	92.52	94.29	92.52	90.48

Table 3: The throughput from one fibre in each ring of the hexabundle is compared at each wavelength band. The slightly worse FRD in the outermost ring results in a small throughput loss.

4. CONCLUSION

The initial results of the new generation of hexabundles has been very successful, and look promising for the successful delivery of Hector I in 2019A. We are currently in the process of building these IFUs in the multiple sizes needed for the instrument, with the final output of 21 hexabundles to be installed into Hector early next year. The manufacturing and assembly process that was developed for the SAMI hexabundles has been built upon to prototype the hexagonally packed hexabundles, and the larger sizes will reach out to 30 arcseconds on sky, ensuring that most galaxies are captured out to $2 R_e$. This will provide clear images of the emission lines and stellar continuum to the outskirts of the galaxies. The regularly packed array, with very high fill factor ensures that the calibrations are extremely reliable and the data reduction simplified beyond that of the current technology. With high throughput and low FRD loss, even where surface brightness is low, these hexabundles will have sufficient light capturing power to accurately measure this. The throughput tests and measurements of FRD have shown that the hexabundles work as effectively as a single bare fibre.

ACKNOWLEDGMENTS

This research was supported by the Australian Research Council Centre of Excellence for All Sky Astrophysics in 3 Dimensions (ASTRO 3D), through project number CE170100013. AHW would like to acknowledge support from an AAO student scholarship. We acknowledge the assistance of Dr Chris Betters with some of the equipment in SAIL.

REFERENCES

- [1] Bland-Hawthorn J., Bryant J. J., Robertson G., Gillingham P., OByrne J., Cecil G., Haynes R., Croom S., Ellis S., Maack M., Skovgaard P., Noordegraaf D, “Hexabundles: imaging fibre arrays for low-light astronomical applications” , Optics Express, 19, 2649 (2011)
- [2] Bryant J. J., O’Byrne J. W., Bland-Hawthorn J., Leon-Saval S. G., “Characterisation of hexabundles: initial results”, MNRAS 415, 2173 (2011)
- [3] Bryant J. J., Bland-Hawthorn J., et al., “SAMI: a new multi-object IFS for the Anglo-Australian Telescope”, SPIE 8446, 250 (2012)
- [4] Bryant J.J., Bland-Hawthorn J., Fogarty L., Lawrence J., Croom S., “Focal ratio degradation in lightly-fused hexabundles”, MNRAS, 438, 869, (2014)
- [5] Bryant J. J. et al., “The SAMI Galaxy Survey: instrument specification and target selection”, MNRAS, 447, 2857 (2015)
- [6] Croom S., et al. “The Sydney-AAO Multi-object Integral field spectrograph (SAMI)”, MNRAS 421, 872 (2012)
- [7] Ramsey L.W., “Focal ratio degradation in optical fibers of astronomical interest”,Fiber optics in astronomy; Proceedings of the Conference, Tucson, AZ, A90-20901 07-35 (1988)
- [8] Haynes et al. (2011)